ACS APPLIED MATERIALS & INTERFACES

Research Article

www.acsami.org

New Synthesis Route of Hydrogel through A Bioinspired Supramolecular Approach: Gelation, Binding Interaction, and in Vitro Dressing

Chieh Cheng, Meng-Che Tang, Chung-Shu Wu, Turibius Simon, and Fu-Hsiang Ko*

Department of Materials Science and Engineering, National Chiao Tung University, 1001 University Road, Hsinchu, Taiwan 300, ROC

Supporting Information

ABSTRACT: Peptide-based supramolecular hydrogels have been comprehensively investigated in biomaterial applications because of their unique bioactivity, biofunctionality, and biocompatible features. However, the presence of organic building blocks in peptide-based hydrogels often results in low mechanical stability. To expand their practical use and range of applications, it is necessary to develop the tool kit available to prepare bioinspired, peptide-based supramolecular hydrogels with improved mechanical stability. In this paper, we present an innovative electrostatic and cross-linking approach in which naphthyl-Phe-Phe-Cys (NapFFC) oligopeptides are combined with gold nanoparticles (AuNPs) and calcium ions (Ca^{2+}) to produce peptide-based supramolecular hydrogels. We further investigate the interactions among NapFFC, AuNPs and Ca^{2+} by microscopy. The morphology of the nanofibrous network constructions and the binding forces exhibited from the hydrogel demonstrated that the combination of two mechanisms successfully enhanced the mechanical stability through the formation of a densely entangled fibrous network of peptide multimers that is attributed to the AuNP linkage and Ca^{2+}-induced agglomeration. UV−vis spectrophotometry and fluorescence analysis were also used to demonstrate the enhanced stability of the hydrogel under various conditions such as thermal, solvent erosion, pH value and sonication. All results indicate that the presence of AuNPs and Ca^{2+} can strengthen the prepared hydrogel by more than doubling the diameter of NapFFC nanofibers, enabling the formation of stronger frameworks and slowing the release of components. Further experiments confirmed that HeLa cells can grow on the bioinspired NapFFC-AuNP hydrogel and exhibit high cell viability and that these cells were killed on contact with a hydrogel containing a drug. Our peptide-based supramolecular hydrogels prepared from the observed electrostatic and cross-linking mechanism exhibited a significantly improved mechanical stability, making them well suited to use as a drug carrier in hydrogel dressings and as extracellular materials (ECMs) for tissue engineering.

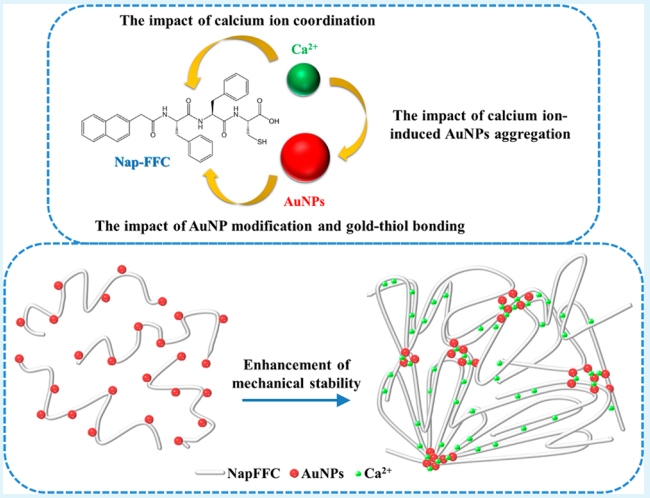

KEYWORDS: *gold nanoparticles, supramolecular, hydrogel, calcium ions, in vitro dressing*

INTRODUCTION

Hydrogels have been widely employed for the food, pharmaceutical, cosmetics, and medicine industries. Besides the current uses, hydrogels have potential future applications in a broad range of medical areas, such as regenerative medicine, tissue engineering, and drug delivery.[1−3] As highly hydrated and porous materials, they can be used as 3D scaffolds for tissue construction and for the control of drug delivery to provide structural integrity and tissue adhesion between a tissue and the surface of material of interest.[4,5] Recently, the study of supramolecular hydrogels consisting of novel low-molecular-weight materials and formed by the self-assembly of simple monomers has rapidly expanded. Contrary to high molecular weight hydrogelators, low molecular weight hydrogelators that form hydrogels generally contain hydrophilic regions, which ensure compatibility with water, and hydrophobic regions, which drive the self-assembly of the peptides in water.[6] Peptides with appropriate hydrophobicity and hydrophilicity can self-assemble into nanofibrous architectures that subsequently entangle to form the matrix of the supramolecular hydrogel. As a new type of soft material,[7] supramolecular hydrogels have attracted considerable research interest because of their useful properties (e.g., rapid responses to physical or chemical stimuli, biocompatibility, and biodegradability) for

Received: June 16, 2015
Accepted: August 14, 2015
Published: August 14, 2015

DOI: 10.1021/acsami.5b05360
ACS Appl. Mater. Interfaces 2015, 7, 19306−19315

Scheme 1. Schematic Diagram Illustrates How the Addition of Components Leads to the Formation of a Densely Entangled Fibrous Network Hydrogel with Enhanced Mechanical Stability

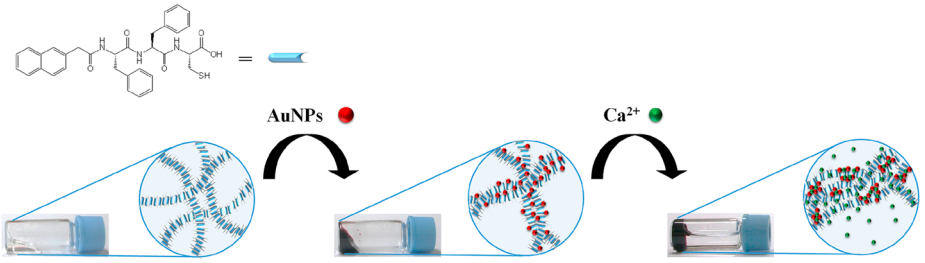

promising applications in biomedicine.[8−10] The three-dimensional network of nanofibers in a molecular hydrogel is porous and allows the incorporation of other bioactive molecules. This makes this new type of biomaterial promising for application in many areas[11] (e.g., tissue engineering,[12] drug delivery,[13] biomaterials,[14] bioanalysis,[15] and chemical sensing[16]). Many of these hydrogels are composed of naturally occurring components such as monosaccharides, nucleic acids and oligopeptides.[17−19] The inherent biological origin of peptides used to form hydrogels makes the hydrogels popular for biological and medical applications, even though one such hydrogel is inspired by peptide interactions seen in Alzheimer's disease.[20] Peptide-based supramolecular hydrogels are advantageous compared to polymeric or biopolymer gels. For example, peptide-based hydrogels combine the advantages of synthetic and naturally derived hydrogels. They can be easily mass produced and combined with chemical and biological elements. Such features allow the design of a particular sequence, as well as the incorporation of functional groups, hence promoting the usability and applicability of these hydrogels.[21] Gazit and coworkers demonstrated that diphenylalanine (FF) peptides self-assembled into nanotubes and applied them as organic light-emitting diodes.[22] Xu et al. described the use of an enzyme transformation to modulate the mode of ligand−receptor binding, which affects the fate of cells.[23] Ulijn et al. designed three diphenylalanine analogues to support the cell proliferation of chondrocytes in cell culture.[24]

However, peptide-based hydrogels composed of small organic building blocks often suffer from low mechanical stability. Although traditional large-molecular-weight hydrogelators (polymeric gels, proteins and polypeptides) focus on the covalent bond, supramolecular chemistry examines the weaker and reversible noncovalent interactions, such as hydrogen bonding, metal coordination, van der Waals forces, electrostatic effects, and $\pi-\pi$ interactions, between molecules.[25,26] Low molecular weight gels tend to break at relatively low strains and are also often reversible, i.e., melting and reforming on warming and cooling, respectively.[6,27] They are highly susceptible to mechanical destruction and solvent erosion, which may cause structural collapse, greatly hindering their practical application. Therefore, the development of hydrogels with rigid structures is necessary and must be addressed. Increasing numbers of reports have been published on the improvement of the mechanical properties of hydrogels. For example, cross-linking methodologies have been developed to increase the nanofiber thickness and to densify the nanofibrous networks, including physical,[28,29] chemical,[30,31] and enzymatic methods.[32,33] The mechanical properties and structural characteristics of hydrogels, such as the degree of cross-linking and the integrity of the gels, can be modulated by the amount and type of cross-linking. Second, metal ions mixed with hydrogelators to form metal−organic nanocomposite hydrogels have also attracted growing interest due to their potential biomaterial applications.[34,35] Incorporation of metal-binding sites into the fibrous assembly structure has been shown to produce stronger hydrogels with new functionalities.[36,37] The interaction between the metal and the organic material arises from the carboxylate moieties, which adopt a range of coordination modes to bridge, chelate, or perform a combination of both. Furthermore, a range of colloidal particles, including carbon-based nanomaterials, inorganic nanoparticles, core−shell nanoparticles and metal/metal-oxide nanoparticles, have been combined with the polymeric network to obtain nanocomposite hydrogels.[38−40] These nanoparticles physically or covalently interact with the polymeric chains, and result in a nanocomposite network with novel properties. In addition, another approach to improve the mechanical strength is to generate anisotropy by the alignment of the nanofibers.[41,42] The majority of these studied methods mentioned above relate to polymeric or macromolecular hydrogels, and there are few research reports concerning the enhancement of the mechanical stability of peptide-based supramolecular hydrogels.[35,42,43] In the present study, to develop a tool kit for the preparation of bioinspired peptide-based supramolecular hydrogels with improved mechanical stability, we propose an electrostatic and cross-linking approach, which is based on synthesized, cysteine-containing peptide supramolecular hydrogelators (NapFFC) integrated with AuNPs and calcium ions as depicted in Scheme 1. Through the use of both metal−organic nanocomposites and a cross-linking method, we attempted to design supramolecular hydrogelators that possess many thiol and carboxylic groups on the supramolecular nanofiber surface as binding sites for the uptake of AuNPs and calcium ions. The positively charged calcium ions induced the agglomeration of the AuNPs, leading to the nanofiber cross-linking reaction, which resulted in the formation of a densely entangled fibrous network that effectively enhanced the mechanical stability of the peptide-based supramolecular hydrogels. Encouragingly, understanding the biomolecular interaction underlying the gelation behavior is of key importance in affinity-based analytics and would be conducive to the possible application of peptide-based hydrogels as functional materials. We also investigate the interaction of NapFFC hydrogelators and AuNPs appended to calcium ions in the self-assembly mechanism. The stable assembled hydrogel retains its high biocompatibility, as well as exhibiting a high degree of physical and chemical stability. We suggest that this favorable approach to improving the mechanical stability of peptide-based hydrogels containing cysteine residues could serve in a variety of technological

DOI: 10.1021/acsami.5b05360
ACS Appl. Mater. Interfaces 2015, 7, 19306−19315

applications in the fields of future biomimetic materials and biotechnology.

EXPERIMENTAL SECTION

Chemicals and Materials. Hydrogen tetrachloroaurate trihydrate ($HAuCl_4 \cdot 3H_2O$), phosphate buffered saline tablets (PBS), sodium carbonate (Na_2CO_3), dimethyl sulfoxide (DMSO), ethanol, and hydrochloric acid (HCl) were purchased from Sigma-Aldrich (St. Louis, MO, USA). Sodium hydroxide (NaOH) was obtained from SHOWA (Chemical Co., Japan). 2-(Naphthalen-6-yl)acetic acid (Nap), L-phenylalanine ($C_9H_{11}NO_2$), *N*-hydroxysuccinimide (NHS), N,N′-dicyclohexylcarbodiimide (DCC), and L-cysteine ($C_3H_7NO_2S$) were purchased from Alfa Aesar (Ward Hill, MA, USA). Chloroform ($CHCl_3$) and sodium citrate dihydrate ($C_6H_5Na_3O_7 \cdot 2H_2O$) were purchased from J. T. Baker (Phillipsburg, NJ, USA). Hydrogen peroxide (H_2O_2) and sulfuric acid (H_2SO_4) were obtained from Merck (Darmstadt, Germany). Dulbecco's modified Eagle medium (DMEM) was obtained from Biowest (Lewes, UK). Tetrazolium salt 3-(4,5-dimethylthiazol-2-yl)-2,5-diphenyltetrazolium bromide (MTT) was obtained from Bersing Bioscience Technology. Trypsin was obtained from Thermo Fisher Scientific (San Jose, CA, USA). HeLa cells were obtained from Bioresource Collection and Research Center (BCRC, Hsinchu, Taiwan). Deionized (DI) water was purified (>18.2 MΩ cm) using a Milli-Q water system (Millipore, Bedford, MA, USA). All other chemicals were guaranteed or analytic grade reagents that were commercially available and used without further purification.

Synthesis of AuNPs. Citrate-stabilized AuNPs were synthesized using the classical Turkevich/Frens procedure.[44,45] A 40 mL aqueous solution consisting of 1 mM $HAuCl_4 \cdot 3H_2O$ was subject to a vigorous boil with stirring in a conical flask, and 38.8 mM sodium citrate (5 mL) was then added rapidly to the solution. The solution was boiled for another 15 min, during which time its color changed from pale yellow to deep red. The solution was cooled to room temperature with continuous stirring. The citrate-stabilized AuNPs appeared to be nearly monodisperse, with an average size of 13.1 ± 1.2 nm.

Synthesis of the NapFFC Hydrogel and NapFFC-AuNPs Nanocomposite. First, 2 mmol of 2-(naphthalen-2-yl)acetic acid, 2 mmol of *N*-hydroxysuccinimide, and 2.1 mmol of N,N′-dicyclohexylcarbodiimide were mixed with chloroform with stirring at room temperature for 4 h and the resulting precipitate was separated by filtration. Second, 2 mmol of L-phenylalanine was dissolved in 8 mL of water containing 4 mmol of Na_2CO_3. After product 2 (in Figure S1) dissolved, 20 mL of acetone was added and the mixture was stirred at room temperature overnight. The solvent was removed and the residue was redissolved in 40 mL of water. Finally, the precipitate was removed by filtration and the filtrate was adjusted to pH 3. The precipitate was collected by filtration and dried in a vacuum. The white powder was used to synthesize NapFF by repeating the same procedure. After the NapFF compounds were obtained, 0.5 mmol NapFF, 0.5 mmol *N*-hydroxysuccinimide, and 0.525 mmol N,N′-dicyclohexylcarbodiimide were added into chloroform, and the mixture stirred at room temperature for 4 h before the resulting precipitate was collected by filtration. Next, 0.5 mmol of L-cysteine was dissolved in 2 mL of water containing 1 mmol of Na_2CO_3.[46] After the solution of product 7 (in Figure S1) was added, the mixture was stirred at room temperature overnight. The solvent was then removed and 40 mL of water was added. Finally, the precipitated product was separated and collected by filtration, and the filtrate was again adjusted to pH 3.

Prior to prepare the NapFFC-AuNP nanocomposites, 5 mg of NapFFC was dissolved in a 1 M NaOH solution and small volumes of 1 M HCl were added to adjust to a pH value of 7 for applications in the biomedical field. Finally, extra DI water was added to achieve a final concentration of 1 wt %. The mixture was then left standing at room temperature for 30 min before being mixed with the AuNP solution to obtain a 0.5 wt % NapFFC-AuNP hydrogel. The NapFFC-AuNP hydrogel was then left standing at room temperature for 1 h before carrying out further experiments.

Physical and Structural Characterization of AuNPs and Nanocomposite Hydrogels. Sizes of the AuNPs were verified by scanning electron microscopy (SEM, JEOL FESEM 6700) and dynamic light scattering (DLS, BECKMAN COULTER Delsa Nano, USA). The morphology of the NapFFC-AuNP nanocomposites was characterized by transmission electron microscopy (TEM, JEOL JEM 100 CX, Japan) and SEM. The chemical structure and bonding type were analyzed by Fourier transform infrared spectroscopy (FT-IR, PerkinElmer Spectrum 100, USA) at a resolution of 1 cm^{-1} using 16 scans for each sample and by NMR (Varian Unity Inova 400, Germany). To study the interactions and mechanical stability of the NapFFC-AuNP hydrogel, 100 μL of hydrogel was added to the bottom of a 1.5 mL glass vial and was left standing at room temperature for 1 h before being treated with 900 μL of various solutions (DI water, PBS buffer or $CaCl_2$ solution) that were added into the glass vial. The components of the hydrogel (NapFFC and AuNPs) were released into the solvent, and the supernatant was collected to detect the released components. NapFFC release was measured using a fluorescence spectrophotometer (Hitachi F-7000, Japan) at 350 PMT voltage, with a 273.0 nm excitation wavelength; the AuNPs were detected by UV−vis absorption spectrophotometry (Hitachi UV-3310) with an absorption wavelength between 400 and 800 nm. Sonication tool (DC300H) used to study the effect of hydrogel stability was purchased from DELTA TAIWAN.

In Vitro Cell Studies. The subcultured HeLa cells were trypsinized, centrifuged, and resuspended in DMEM medium in advance. Two hundred microliters of the NapFFC-AuNP hydrogel was spread on half of a clean 15 cm cell culture dish to form a transparent thin film, and the same amount of DOX encapsulating hydrogel was also spread on the dish. After 1 h, a $CaCl_2$ solution was added to treat the hydrogel for 30 min before the hydrogel was washed with a PBS buffer solution 3 times. After being prepared and treated with a $CaCl_2$ solution, the HeLa cells were added into the cell culture dish. Ten milliliters of DMEM supplemented with 10% fetal bovine serum and 1% penicillin-streptomycin was then added to the dish. The culture was then incubated in a humidified atmosphere containing 5% CO_2 at 37 °C. After 24 h incubation, the cell morphology was observed under a bright microscope. The cell viability was characterized by incubating cells with the MTT reagent for 4 h.

RESULTS AND DISCUSSION

Gelation Properties of the NapFFC-AuNPs Hydrogel. In this study, to form nanocomposites with AuNPs, we synthesized a cysteine amino acid on the terminus of NapFF to form the compound NapFFC. Figure S1 illustrates the synthetic route and chemical structure of NapFFC. The NMR data (Figure S2) suggests that the chemical structure of NapFFC synthesized via this synthetic route is successfully obtained. Hence, we can use this compound to carry out the follow-up experiment. As widely reported, the self-assembly of amphiphilic peptides such as Nap-Phe-Phe-OH (NapFF), the protected form of H-Phe-Phe-OH, have been studied extensively.[10,25,26] NapFFC can also effectively self-assemble into nanotubes in water to form nanofibrils because of the π−π stacking of the aromatic residues and other hydrophobic interactions. The gelation properties of NapFFC in DI water at pH 7.4 is shown in Figure 1A and Figure S3. The NapFFC solution was prepared using various Nap-FFC concentrations from 0.2 to 1.0 wt % to investigate the gelation properties. According to the optical images, the Nap-FFC solution remained in the liquid phase at low concentrations, but at increased Nap-FFC concentrations, the Nap-FFC solution became more viscous. At a concentration of 1.0 wt %, the Nap-FFC solution formed a complete rigid hydrogel. In general, increasing the peptide concentration leads to the formation of an entangled fibrous network at the microscopic level, resulting in the formation of supramolecular hydrogels on the macroscopic level.

DOI: 10.1021/acsami.5b05360
ACS Appl. Mater. Interfaces 2015, 7, 19306−19315

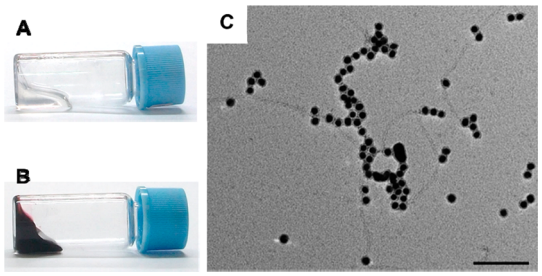

Figure 1. Optical images showing gelation properties of (A) 0.5% NapFFC in DI water at pH 7.4, and (B) NapFFC-AuNPs in DI water at pH 7.4. (C) TEM image showing the NapFFC-AuNP hydrogel (NapFFC = 0.5%; AuNPs = 200 nM). The scale bar indicates 100 nm.

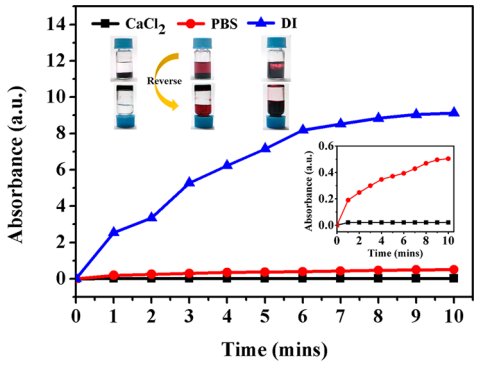

Figure 2. Effect of AuNPs release from UV−vis absorption spectra of the NapFFC-AuNP hydrogel in various solvents ($CaCl_2$, PBS, and DI water). The hydrogels resided at the bottom of the vial and were inverted (optical images).

Based on the verified supramolecular properties of Nap-FFC hydrogels, gelation of the Nap-FFC-AuNPs is discussed in relation to the following experiments. First, AuNPs were synthesized by a hydrothermal process and the particle size distribution characterized by SEM (Figure S4). The AuNPs had a mean diameter of 13.1 nm. Similar results were observed by dynamic light scattering, with a diameter of 13.16 nm obtained (Figure S5). The uniform AuNPs prepared were then used to investigate the gelation properties of NapFFC-AuNPs in terms of their organization into supramolecular entities. In this experiment, the NapFFC powder was dissolved in DI water ([NapFFC] = 0.5 wt %, pH 7.4) and then mixed with AuNP solutions of various concentrations (0, 120, 300, 600, 900, 1200 nM). As shown in Figures 1B and Figure S6, NapFFC-AuNP nanocomposites are able to form hydrogels due to the self-assembly of the NapFFC and AuNPs. The optical images clearly show that the interaction between the AuNPs and NapFFC resulted in increased strength and viscosity at different AuNP concentrations (0, 120, 300, 600, 900, 1200 nM). The viscous liquid phase and weak hydrogel was observed at low concentrations of AuNPs (120 and 300 nM). In contrast, the NapFFC-AuNPs formed stronger hydrogels at higher concentrations of AuNPs (600, 900, and 1200 nM). Thus, it can be seen that the introduction of AuNPs can alter the gelling properties of the NapFFC-AuNP hydrogel. This phenomenon is a typical gelation process mediated by Au-thiol bonding and carboxyl noncovalent interactions of stimuli-responsive supramolecules with AuNPs. Instead of dispersing randomly in the hydrogel, notable evidence was found using TEM (Figure 1C) that the AuNPs bind to the nanofibers that tend to form the NapFFC supramolecule by self-assembly. Based on this phenomenon, the nanofibers-AuNPs exhibited an enhanced mechanical stability in the NapFFC-AuNP nanocomposites because of the densely intermingled networks of cross-linked nanofibers that are formed.

Effect of Different Solvents. Considering that the stability of the cross-linked hydrogels often changes with the environment, the influence of the solvent was also investigated in this work. The NapFFC-AuNP hydrogel was immersed in various solvents (DI water, PBS and $CaCl_2$ solution) as demonstrated in Figure 2. The NapFFC-AuNP hydrogel was exposed to different solvents for 10 min. The UV−vis absorption spectrum demonstrated that numerous AuNPs were released into the DI water, and the hydrogel was unstable and deformed (Figure 2, inset optical image). In the PBS condition, the solid NapFFC-AuNP hydrogel remained at the bottom of the vial in good shape, but the optical image and UV−vis absorption spectra (inset) indicate that some AuNPs diffused into the PBS solution during the 10 min period of exposure. Interestingly, the NapFFC-AuNP hydrogel maintained its shape and produced a clear supernatant in 200 mM $CaCl_2$, which was in contrast with the results obtained with the other investigated solvents. The UV−vis absorption spectrum showed that no AuNPs were released into solution in the presence of $CaCl_2$. These results indicated that a stable and rigid hydrogel was formed. The NapFFC-AuNP hydrogel exhibited excellent mechanical properties under the $CaCl_2$ conditions. We expect that this observed behavior is due to the Ca^{2+} present in the hydrogel, which restricts the release of negatively charged AuNPs into solution. Therefore, this phenomenon prevents the NapFFC-AuNP nanocomposite from detaching from the bottom of vial, which indirectly promotes the mechanical properties of the hydrogel.

Interaction between NapFFC-AuNPs and Calcium Ions. In the experiments described above, the NapFFC-AuNP hydrogel exhibited excellent mechanical properties under $CaCl_2$ conditions. To the best of our knowledge, this is the first report to mention the playing role of calcium ion for the hydrogel-based materials. Generally, calcium is one of the most abundant cations present in living organisms. It is the main cation present in the mineral phase of bone and is involved in the control of many important physiological functions, such as muscle contraction. Therefore, in this context, whether calcium ions are the key component in the assembly of the NapFFC-AuNP hydrogel should be clearly investigated. First, UV−vis absorption spectroscopy was used to determine how the concentration of Ca^{2+} influenced the NapFFC-AuNP hydrogel formed. In Figure 3, the AuNPs that modified and encapsulated the NapFFC nanofibrous hydrogel were still released into solution at low Ca^{2+} concentrations (0.02, 0.2, and 2 mM) but formed more stable hydrogels at the bottom of the vial at high Ca^{2+} concentrations (200 mM). In other words, under Ca^{2+}-rich conditions, the solution separates obviously, in which the dark-red gel observed is due to the agglomeration induced by charge effect, with a transparent supernatant (Inset). On the contrary, weak forces cannot afford to form a stable hydrogel, and this situation results in the release of NapFFC-AuNPs into the solution. As a result, the stoichiometry of NapFFC-AuNP hydrogel and Ca^{2+}-rich conditions play an important role on mechanical property of hydrogel-related materials.

After confirming that a high Ca^{2+} concentration influences the NapFFC-AuNP hydrogel stability, microscopic observation

DOI: 10.1021/acsami.5b05360
ACS Appl. Mater. Interfaces 2015, 7, 19306−19315

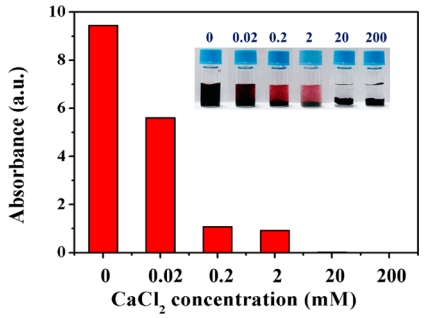

Figure 3. UV−vis absorption spectra of the NapFFC-AuNP hydrogel solutions in different concentrations (0, 0.02, 0.2, 2, 20, and 200 mM) of $CaCl_2$. The data suggested the degree to which the AuNPs were released, determined from the absorption maximum (A_{520}).

of the supramolecular assembly was used for further confirmation. From the microscopic perspective, the key factors that determine the mechanical properties of hydrogels are based on the bonding strength among the supramolecular hydrogel components, the average thickness of the nanofibers and the cross-linking density of the fibrous networks.[43,47] To obtain greater insight into the assembly process and stabilizing interactions, we attempted to form a hydrogel with the addition of AuNPs or Ca^{2+} to compare the width of nanofibers that formed. As shown in Figure 4, examination of the lower critical gelation concentration (0.5 wt %) revealed that the NapFFC molecules self-assemble to produce uniform, long nanofibers with diameters of 12.51 ± 3.56 nm in DI water at pH 7.4. These nanofibers entangle to form the low density network and afford a transparent hydrogel (Figure 4A). Using a similar method, we prepared a NapFFC-AuNP nanocomposite hydrogel. Figure 4B illustrates the morphology of a 0.5 wt % NapFFC-AuNP nanocomposite with a dense fibrous structure. The diameters of the NapFFC nanofibers were 28.76 ± 2.12 nm. There were many 13.1 nm AuNPs that adhered to the nanofibers with a good dispersity as shown in the aforementioned TEM image (Figure 1C). The observed thickening of the fibers substantiates supports our speculation that the AuNPs enhance the mechanical strength and stability of the hydrogel effectively. The diameter of the 0.5 wt % NapFFC nanofibers was 25.38 ± 2.34 nm after treatment with 200 mM $CaCl_2$ (Figure 4C). Interestingly, the modification with either the AuNPs or by the treatment with $CaCl_2$ can increase the diameters of the NapFFC nanofibers obtained. Figure 4D shows the morphology of the 0.5 wt % NapFFC-AuNP hydrogel treated with a 200 mM $CaCl_2$ solution. Under these conditions, both the AuNPs and $CaCl_2$ elements were added to the NapFFC hydrogel, and the nanofiber diameter increased to 55.48 ± 6.27 nm. In addition, the 13.1 nm AuNPs that adhered onto the nanofibers were conspicuously densified. We suggest that such an observed change in the fiber diameter in response to an increase results from a charge-induced phenomenon. The AuNPs with negatively charged surface (Zeta potential: −38.8 mV) aggregate due to the positively charged calcium ions, resulting in the observed AuNP densification and agglomeration behavior. The AuNPs that were previously incorporated on the nanofiber surface through a cysteine group promoted the densification of NapFFC nanofibers upon Ca^{2+} treatment, which ultimately contributes to the phenomenon of increased fiber diameters. To further investigate the key role of calcium ions, we further examined the calcium sites and interactions between the calcium ions and the organic molecules by FT-IR spectroscopy. The main mechanism of calcium interaction with organic molecules is based on calcium coordination with the carboxylate group. Figure 4E shows representative FT-IR spectra of pure NapFFC, NapFFC-AuNPs, NapFFC-Ca^{2+} and NapFFC-AuNPs-Ca^{2+}. According to previous publication, they reported that the ligand bands at 3300, 1705, 1390, 1290, and 918 cm^{-1} could be assigned to O−H stretch, C═O stretch, C−O stretch, and O−H bending vibrations, respectively. The bands at 3280, 1637, 1528, and 1221 cm^{-1} can be assigned to the amide A, amide I, amide II, and amide III vibrations, respectively. The band at 1690 cm^{-1} can be attributed to the C═O vibration of the carbamate moiety.[35] However, the variation in C═O absorption occurs at 1644 cm^{-1} from our experiment in Figure 4E. This phenomenon is ascribed to the amide functional groups of NapFFC; the C═O group of an amide vibrates at an lower frequency, 1640−1680 cm^{-1}.[48] As in the previous work by Alexandre Mantion and co-workers, the amide band positions are indicative of a β-sheet structure which also results in the shift of C═O absorption.[49] IR indicates that the β-sheet is conserved after the reaction with calcium and copper,

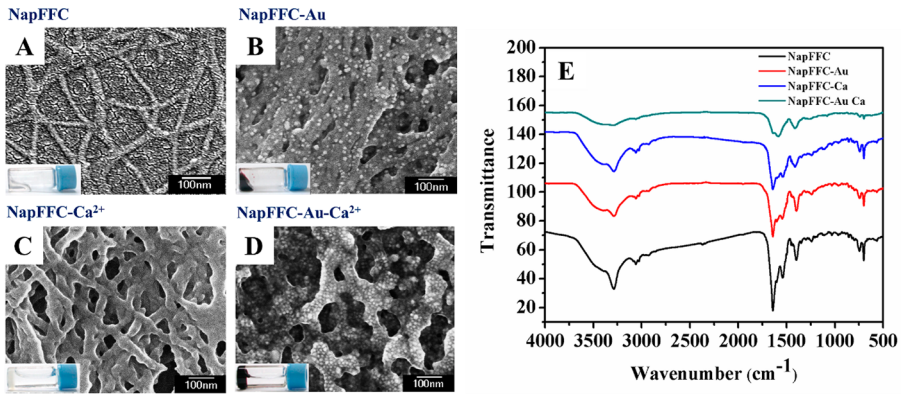

Figure 4. SEM micrographs of the (A) NapFFC nanofibrous hydrogel, (B) NapFFC-AuNP nanofibrous hydrogel, (C) NapFFC nanofibrous hydrogel immersed in 200 mM $CaCl_2$, and (D) NapFFC-AuNP nanofibrous hydrogel immersed in 200 mM $CaCl_2$. The pH value of each sample was controlled at 7.4. (E) FT-IR spectra of the NapFFC carboxylate group interaction with the metal and metal ions. NapFFC (black line), NapFFC-AuNP nanocomposites (red line), NapFFC treated with 200 mM $CaCl_2$ (blue line), and NapFFC-AuNP nanocomposites treated with 200 mM $CaCl_2$ (green line), respectively.

DOI: 10.1021/acsami.5b05360
ACS Appl. Mater. Interfaces 2015, 7, 19306−19315

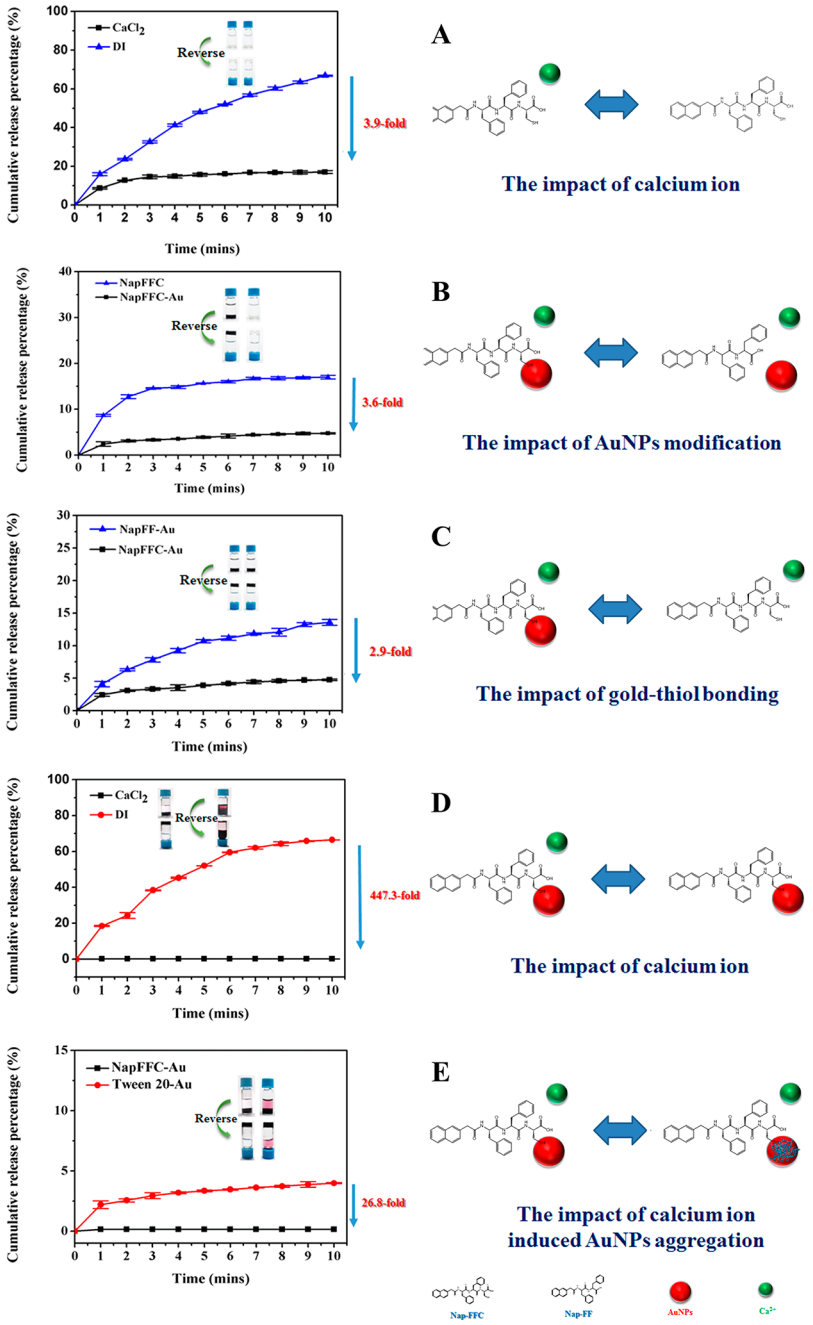

Figure 5. Interaction analysis by the cumulative percentage of the NapFFC compound released and AuNPs released detected by fluorescence and UV−vis spectrophotometry, respectively. (A) Impact of calcium ions on the NapFFC hydrogel. (B) Impact of the AuNP modification on the NapFFC-AuNP hydrogel. (C) Impact of gold−thiol binding on the NapFFC-AuNP hydrogel. (D) Impact of the calcium ions on the NapFFC-AuNP hydrogel. (E) Impact of calcium ion-induced agglomeration of AuNPs.

because the two bands at 1628, and 1533 cm^{-1}, which are indicative of the β-sheet, are still visible in the crystalline precipitates. In our case, the β-sheet structure was still existed, and the IR also shows differences between the pure peptide and the metal complexes of NapFFC-AuNPs, NapFFC-Ca^{2+} and NapFFC-AuNPs-Ca^{2+}. After reaction of the ligand with the AuNPs and calcium ions, the C═O stretch at 1644 cm^{-1} and the O−H stretch at 3300 cm^{-1} of the cysteine carboxylate group disappeared. This is consistent with the interaction between the ligand and metal ion via the carboxylic acid moiety.[50] Finally, the FT-IR spectrum suggests that the carboxylic acid acts as a bridging unit between the metal centers in the NapFFC-AuNP hydrogel.

Interaction Investigation of NapFFC, AuNPs, and Calcium Ions. As indicated in the previous experiments, the rigid hydrogel components interact with one another and have synergistic impact on the properties of the formed hydrogel. To explore the effect of each component on the rigid hydrogel, including the AuNP modification of NapFFC, gold−thiol bonding, calcium ion coordination with the NapFFC carboxylate group, and the calcium ion inducing the AuNP agglomeration, we investigated five conditions (Figure 5). As indicated in Figure 5A, the influence of calcium ions alone on

DOI: 10.1021/acsami.5b05360
ACS Appl. Mater. Interfaces 2015, 7, 19306−19315

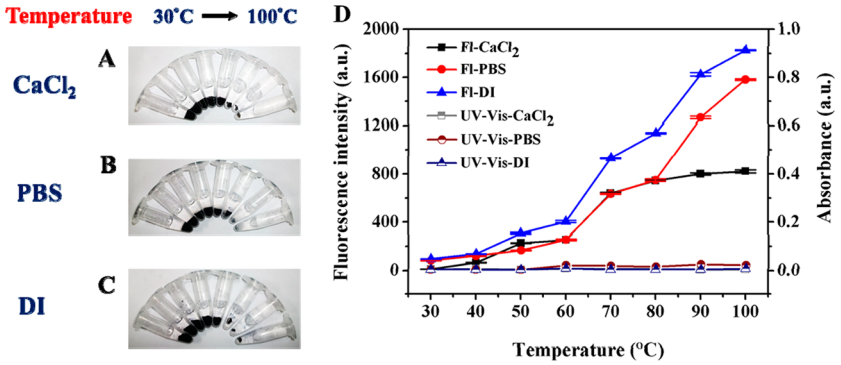

Figure 6. Thermal stability of the hydrogel in various solutions from 30 to 100 °C. (A) $CaCl_2$, (B) PBS buffer, and (C) DI water. Each of the experimental NapFFC-AuNP nanocomposite hydrogel samples was treated with $CaCl_2$ for 10 min prior to immersion in the various solutions. (D) Chart of the UV−vis absorption spectra showing AuNP release and the fluorescence spectra of the NapFFC compound in various solutions at different temperatures.

the NapFFC hydrogel was probed. Considering the fluorescence of NapFFC, the percentage released from the NapFFC hydrogel through diffusion into the DI water was determined. In this experiment, we added DI water and a $CaCl_2$ solution to a 0.5 wt % NapFFC hydrogel. The fluorescence data shows that the addition of calcium ions resulted in a 3.9-fold reduction in the quantity of NapFFC released in a 10 min period. As expected, the addition of calcium ions was observed to slow the release tendency. In other words, the release quantity was limited by enhancing the mechanical stability, which could be attributed to the calcium ions that interact with the carboxylate moieties the supramolecular hydrogelators provided. To further investigate the diversity of the components, we then explored the AuNPs. The impact of the AuNP modification on the hydrogel is illustrated in Figure 5B. In the case where calcium ions were added to both the NapFFC-AuNP hydrogel and the control, it was found that the NapFFC hydrogel with 600 nM AuNPs added exhibited a 3.6-fold decrease in NapFFC release compared with the hydrogel without AuNPs in a 10 min period. The NapFFC-AuNP hydrogel was stable at the bottom of the vial, and no red color was observed, indicating that there was no diffusion of the AuNPs into the supernatant (see inset photograph in Figure 5B). Notably, on the basis of these results, the release behavior exhibited a saturation, which was approached quickly after 3 min whether AuNPs were present or not. Furthermore, when compared with the hydrogel treated with calcium ions alone, the release percentage decreased from 16% to below 5% when AuNPs were added. This observation demonstrates that AuNPs play another important role in the enhancement of the mechanical stability. In fact, there are multiple and complex interactions between the NapFFC and AuNPs, including OH-AuNPs, COOH-AuNPs, NH-AuNPs, and SH-AuNPs. Herein, the SH-AuNPs (gold−thiol binding) interaction is recognized as the most powerful force because it is covalent in nature. Therefore, the extent of the competitive binding among various interactions between AuNPs and the hydrogelator was also investigated in depth. For this purpose, the NapFF peptide that lacks the cysteine amino acid was synthesized to compare with the NapFFC peptide; both the NapFF and NapFFC hydrogel were mixed with AuNPs to form rigid nanocomposites as shown in Figure 5C. As predicted, the NapFFC with gold−thiol binding was more effective in strengthening the hydrogel and restricting component release. The gold−thiol binding decreased the quantity released of NapFFC by 2.9-fold in a 10 min period. This result indicates that the affinity between the hydrogelator and AuNPs needs to be taken into account. To summarize the above results, the calcium treatment has a significant influence on restraining the release of NapFFC compounds into solution; the modification of AuNPs with NapFFC to form NapFFC-AuNP nanocomposites through gold−thiol bonding improved the mechanical stability further.

To further explore the influence of the calcium ions on the NapFFC-AuNP hydrogel, we determined the cumulative percentage of AuNPs released using UV−vis absorption spectrophotometry to examine whether any AuNPs escaped from the prepared hydrogel. In contrast with the experiments shown in Figure 5A, the NapFFC was modified with the AuNPs before treating with $CaCl_2$, instead of adding calcium ions only. In comparison with the treatment with the $CaCl_2$ solution and DI water, the NapFFC-AuNPs strengthened the mechanical properties of the hydrogel without releasing components into solution only in the presence of calcium ions (Figure 5D). As seen in the inset photograph of Figure 5D, the NapFFC-AuNP hydrogel without added calcium ions diffused into the DI water and the color of the solution turned red. This means that the interactions between the AuNP-modified NapFFC nanofibers was not strong enough, resulting in the diffusion of the components into the DI after 10 min. This phenomenon demonstrates that the AuNPs make the distance between the NapFFC nanofibers closer, but this force is insufficient to make a robust hydrogel. In contrast, calcium ions can help make the AuNP-modified hydrogel more stable. However, how the calcium ions affect the need for robust hydrogels requires discussion in detail. In the SEM image shown in Figure 4D, we observe the AuNP densification on the nanofiber surface after treatment with $CaCl_2$. We suggested this phenomenon arises because of the positively charged calcium ions inducing the agglomeration of the surface-negatively charged AuNPs. To investigate the impact of the calcium ions on the agglomeration of AuNPs, we modified the AuNP surface with Tween-20 as a protective layer in advance to prevent the positive charge of the calcium ions from inducing agglomeration. The appearance of a red color is clearly seen in the $CaCl_2$ solution in the inserted optical image shown in Figure 5E. The AuNPs diffused into the $CaCl_2$ solution instead of congregating within the hydrogel at the bottom of the vial. However, the hydrogel still formed a rigid block, despite the release of AuNPs. We can infer from this experiment that the induced agglomeration reduced the release of AuNPs by 26.8-fold and

DOI: 10.1021/acsami.5b05360
ACS Appl. Mater. Interfaces 2015, 7, 19306−19315

represents the important interaction in our proposed hydrogel. Based on these results, the Ca^{2+} influences both the NapFFC nanofiber and AuNP distribution. The calcium ions coordinate with the NapFFC carboxylate groups as connectors, and induce the agglomeration of AuNPs. In summary, AuNPs and calcium ions have a mutual and synergistic impact on and interaction with NapFFC. A rigid hydrogel is obtained only when both are present. All of these interactions result in increasing nanofiber widths, which is consistent with the aforementioned results (Figure 4).

Stability of the Prepared Hydrogel under Various Temperatures, pH Conditions, and Sonication Endurance. Thermal stability is an important property of hydrogelators that have wide applications in a number of biomedical fields. In this experiment, the thermal stability of the rigid hydrogel was found to depend on the quantity of NapFFC-AuNPs released. Figure 6 illustrates the results, in which the NapFFC-AuNP hydrogel was treated with $CaCl_2$ for 10 min before being immersed in various solvents, including DI water, PBS, and $CaCl_2$, for a further 10 min. Optical images were then taken (Figure 6A–C). From 30 to 60 °C, the hydrogel maintained an almost identical appearance. When the temperature exceeded 70 °C, the hydrogel contracted. The observation of contraction effect may be attributed to the agglomeration of AuNPs that become unstable and tend to aggregate at high temperature. The supernatant solutions were also examined using fluorescence and UV–vis adsorption spectrometry. As illustrated in Figure 6D, some NapFFC was detected above 70 °C. The aromatic–aromatic interactions between the NapFFC molecules weakens with increasing temperature, allowing NapFFC to diffuse into the supernatant. However, the addition of Ca^{2+} to the NapFFC-AuNP hydrogel causes an irreversible reaction, such that the diffusion was considered to be typical due to its low proportion (approximately 10%). In addition, after heating in a water bath, the UV–vis absorption spectra confirmed that no AuNPs were released as a result of treating with Ca^{2+} in advance; the result is the same as that shown in Figure 2. This observation validates the aforementioned statement concerning the agglomeration of the AuNPs. Therefore, Ca^{2+} treated NapFFC-AuNP hydrogels have good thermal stability in different solvents below 60 °C because the Ca^{2+} effectively restricts the release of the negatively charged AuNPs into solution, which prevents the NapFFC-AuNP nanocomposite from detaching from the bottom of the Eppendorf, which indirectly promotes the mechanical properties of the hydrogel. Furthermore, the Ca^{2+} containing solvent further interacts with the NapFFC nanofibers and protects the rigid gel to preserve its form at high temperatures. In addition to thermal stability, pH stability and sonication endurance are also significant indices of hydrogelators in application to biomedical fields. As Figure S7 suggests, the prepared hydrogel exhibits good pH stability in the range of 4–10 under room temperature. Despite slight detachment from the bottom of the Eppendorf below pH 5, the NapFFC-AuNP hydrogel maintains its shape and no AuNP in the supernatant was observed from UV–vis spectrophotometry. In alkaline environments, the dark-red hydrogel still performs good stability. Besides, Figure S8 reveals the release of little amount of NapFFC and no AuNP after exposure to the sonication for 10 min. Consequently, the NapFFC-AuNP nanocomposite hydrogel maintains its robustness regardless of which solution was used, as long as the hydrogel was treated with Ca2+ in advance. As a result, such an outstanding stability of the hydrogel under different rigorous conditions confirms them suitable for biotechnological applications.

Cytotoxicity Performance and Drug Encapsulation. To support the use of the NapFFC-AuNP nanocomposite hydrogel in drug delivery or in the tissue engineering field, the biological safety of this novel material was investigated. The cell viability test is necessary to confirm the cytotoxicity of the NapFFC-AuNP nanocomposites. The biocompatibility of the NapFFC-AuNP nanocomposites was evaluated as nontoxic in human cells (HeLa cells) by MTT assays. HeLa cells were exposed to different concentrations (20, 50, 100, 200, 500 μM) of the NapFFC-AuNP nanocomposites for 24, 48, and 72 h. As shown in Figure 7, after a 24 h incubation, no toxic effect was

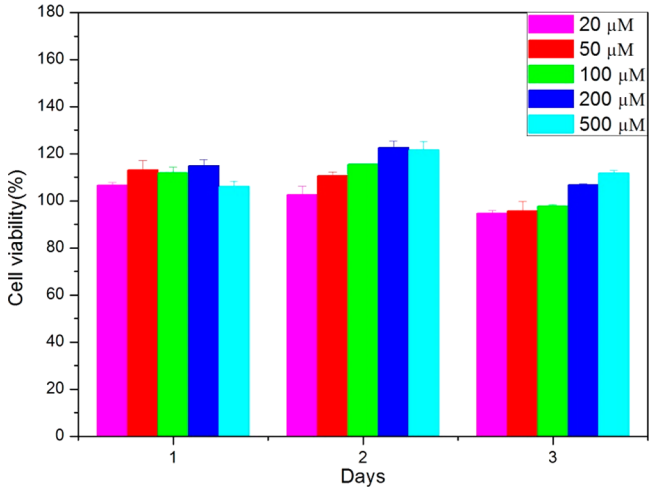

Figure 7. Cytotoxicity of the NapFFC-AuNP nanocomposites in MTT assays. The relative cell viability of HeLa cells incubated with different concentrations (20, 50, 100, 200, 500 μM) of NapFFC-AuNP nanocomposites for 24, 48, and 72 h. Each data point results from at least three independent experiments.

observed on the HeLa cells at any concentration. Similar results were observed after 48 h with near or greater than 100% cell viability at all NapFFC-AuNP nanocomposite concentrations tested. A small decrease was observed in the percent viability only after 3 days of incubation. As a whole, the obtained results demonstrate that the novel nanocomposite hydrogel material will not be toxic in vitro.

Intrigued by the proven noncytotoxicity, we sought to study the capability of the NapFFC-AuNP hydrogel to encapsulate drugs in biomedical dressing applications. With similar robustness and biocompatibility to those of extracellular matrix (ECM), the NapFFC-AuNP nanocomposites can effectively form rigid hydrogels that resist mechanical destruction and solvent erosion after $CaCl_2$ treatment. In this experiment, the NapFFC-AuNP nanocomposite hydrogels were spread out smoothly on the bottom of half a Petri dish (left side) with a $CaCl_2$ treatment and hydrogels containing the anticancer drug DOX at concentrations of 0, 50 μM, and 100 μM were prepared in Figure 8. Figure 8A was a control experiment. In Figure 8B, the optical image suggests visually that there were few surviving HeLa cells on the gel (left side), but there were many healthy cells on the nongel area (right side). Furthermore, on increasing the concentration of encapsulated DOX, no surviving cells were found (Figure 8C). Conversely, the control experiment involving HeLa cells incubated on the

DOI: 10.1021/acsami.5b05360
ACS Appl. Mater. Interfaces 2015, 7, 19306–19315

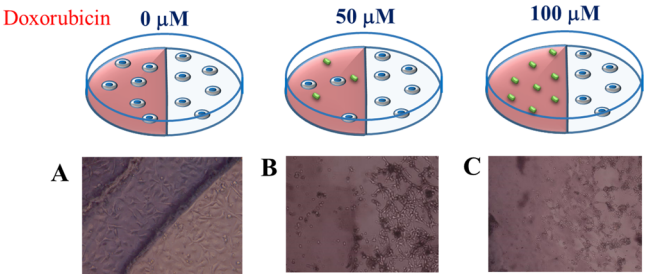

Figure 8. In vitro drug delivery test on the nanocomposite hydrogel (right side, nongel; left side, gel). (A) Optical images of HeLa cells grown on the NapFFC-AuNP nanocomposite hydrogel. Incubation of HeLa cells on the NapFFC-AuNP hydrogel containing DOX at a concentration of (B) 50 and (C) 100 μM.

nanocomposite hydrogels demonstrated identical normal growth to that of the other half of the plate without the gel (Figure 8A). In general, the cell viability gradually decreased as the concentration of DOX increased and the cell survival ratio was very low when the concentration of DOX was over 5 μg/mL (Figure S9). The obtained results imply that the cellular toxicity toward HeLa cells incubated on the DOX encapsulating, mechanical-stability-enhanced NapFFC-AuNP hydrogel originates from the release of DOX molecules inside cells. Despite being incubated on one plate, the cells still survive on the nongel area, whereas the HeLa cells cannot exist on the hydrogel containing the DOX area. This observation confirms that only cells attached directly to the gel can interact with the DOX, resulting in cell death. We can speculate that the drug molecules cannot easily diffuse into the culture medium because they are well-captured within the hydrogel. Because of this outstanding performance, NapFFC-AuNP nanocomposite hydrogels have great potential in tissue engineering. To summarize the above characteristics, NapFFC-AuNP nanocomposite hydrogels treated with $CaCl_2$ are effective carriers for drug delivery and simultaneously have the potential to be applied in future tissue engineering.

CONCLUSIONS

In conclusion, we have synthesized a new peptide-based supramolecular hydrogel with cysteine (NapFFC) and report that the addition of both AuNPs and Ca^{2+} to the low molecular weight gelator results in the enhancement of the mechanical stability of the hydrogel based on a novel electrostatic and cross-linking approach. The NapFFC hydrogels incorporate AuNPs, the characteristics of which were revealed by microscopy, and these robust hydrogels exhibit a broadened nanofibrous network derived from NapFFC linked to AuNPs. The hydrogels also incorporate Ca^{2+}, suggesting that the coalescence of both metal−organic nanocomposites and cross-linking methods efficiently promote an increase in nanofiber thickness and densification of the nanofibrous network. The interactions between the NapFFC, AuNPs and Ca^{2+} were analyzed using optical microscopy, UV−vis, fluorescence spectrophotometry and FT-IR clarified that the Ca^{2+} interacts with the carboxylic acid of the NapFFC. Such a unique hydrogel architecture also exhibited good stability under various aqueous, thermal and sonication conditions. This demonstrates that the prepared hydrogels exhibit enhanced mechanical property due to synergistic effect. Furthermore, this peptide-based supramolecular hydrogel with high biocompatibility served as a carrier for drug encapsulation for an in vitro dressing. The superior drug-encapsulating capability and release behavior of the hydrogel makes it a promising candidate for the future generation of bioactive nanocomposites that could be used in drug-delivery dressings and extensively exploited in biomedical and tissue engineering applications.

ASSOCIATED CONTENT

Supporting Information

The Supporting Information is available free of charge on the ACS Publications website at DOI: 10.1021/acsami.5b05360.

Additional information as noted in text (PDF)

AUTHOR INFORMATION

Corresponding Author

*Phone: +886-35712121, ext 55803. E-mail: fhko@mail.nctu.edu.tw.

Notes

The authors declare no competing financial interest.

ACKNOWLEDGMENTS

This investigation was supported by fund provided by the Ministry of Science and Technology (MOST 104-2113-M-009-008-MY3).

REFERENCES

(1) Apostolov, A. A.; Boneva, D.; Vassileva, E.; Mark, J. E.; Fakirov, S. Mechanical Properties of Native and Crosslinked Gelatins in a Bending Deformation. *J. Appl. Polym. Sci.* **2000**, *76*, 2041−2048.

(2) Seliktar, D. Designing Cell-Compatible Hydrogels for Biomedical Applications. *Science* **2012**, *336*, 1124−1128.

(3) Mckay, C. A.; Pomrenke, R. D.; McLane, J. S.; Schaub, N. J.; DeSimone, E. K.; Ligon, L. A.; Gilbert, R. J. An Injectable, Calcium Responsive Composite Hydrogel for the Treatment of Acute Spinal Cord Injury. *ACS Appl. Mater. Interfaces* **2014**, *6*, 1424−1438.

(4) Brandon, V. S.; Shahana, S. K.; Omar, Z. F.; Ali, K.; Nicholas, A. P. Hydrogels in Regenerative Medicine. *Adv. Mater.* **2009**, *21*, 3307−3329.

(5) Xavier, J. R.; Thakur, T.; Desai, P.; Jaiswal, M. K.; Sears, N.; Cosgriff-Hernandez, E.; Kaunas, R.; Gaharwar, A. K. Bioactive Nanoengineered Hydrogels for Bone Tissue Engineering: A Growth-Factor-Free Approach. *ACS Nano* **2015**, *9*, 3109−3118.

(6) Raeburn, J.; Zamith Cardoso, A.; Adams, D. J. The Importance of the Self-Assembly Process to Control Mechanical Properties of Low Molecular Weight Hydrogels. *Chem. Soc. Rev.* **2013**, *42*, 5143−5156.

(7) Lin, D. C.; Horkay, F. Nanomechanics of Polymer Gels and Biological Tissues: A Critical Review of Analytical Approaches in the Hertzian Regime and Beyond. *Soft Matter* **2008**, *4*, 669−682.

(8) De Loos, M.; Van Esch, J.; Kellogg, R. M.; Feringa, B. L. Chiral Recognition in bis-Urea-Based Aggregates and Organogels through Cooperative Interactions. *Angew. Chem., Int. Ed.* **2001**, *40*, 613−616.

(9) Yang, Y.; Suzuki, M.; Shirai, H.; Kurose, A.; Hanabusa, K. Nanofiberization of Inner Helical Mesoporous Silica Using Chiral Gelator as Template under a Shear Flow. *Chem. Commun.* **2005**, *15*, 2032−2034.

(10) Yang, Z.; Liang, G.; Wang, L.; Xu, B. Using a Kinase/Phosphatase Switch to Regulate a Supramolecular Hydrogel and Forming the Supramolecular Hydrogel *in Vivo*. *J. Am. Chem. Soc.* **2006**, *128*, 3038−3043.

(11) Rabotyagova, O. S.; Cebe, P.; Kaplan, D. L. Protein-Based Block Copolymers. *Biomacromolecules* **2011**, *12*, 269−289.

(12) Panda, J. J.; Dua, R.; Mishra, A.; Mittra, B.; Chauhan, V. S. 3D Cell Growth and Proliferation on a RGD Functionalized Nanofibrillar Hydrogel Based on a Conformationally Restricted Residue Containing Dipeptide. *ACS Appl. Mater. Interfaces* **2010**, *2*, 2839−2849.

DOI: 10.1021/acsami.5b05360
ACS Appl. Mater. Interfaces 2015, 7, 19306−19315

(13) Xu, X. D.; Liang, L.; Chen, C. S.; Lu, B.; Wang, N. L.; Jiang, F. G.; Zhang, X. Z.; Zhuo, R. X. Peptide Hydrogel as an Intraocular Drug Delivery System for Inhibition of Postoperative Scarring Formation. *ACS Appl. Mater. Interfaces* **2010**, *2*, 2663−2671.
(14) Vandermeulen, G. W. M.; Klok, H. A. Peptide/Protein Hybrid Materials: Enhanced Control of Structure and Improved Performance through Conjugation of Biological and Synthetic Polymers. *Macromol. Biosci.* **2004**, *4*, 383−398.
(15) Kiyonaka, S.; Sada, K.; Yoshimura, I.; Shinkai, S.; Kato, N.; Hamachi, I. Semi-Wet Peptide/Protein Array Using Supramolecular Hydrogel. *Nat. Mater.* **2004**, *3*, 58−64.
(16) Yamguchi, S.; Yoshimura, I.; Kohira, T.; Tamaru, S.; Hamachi, I. Cooperation between Artificial Receptors and Supramolecular Hydrogels for Sensing and Discriminating Phosphate Derivatives. *J. Am. Chem. Soc.* **2005**, *127*, 11835−11841.
(17) De la Rica, R.; Matsui, H. Applications of Peptide and Protein-Based Materials in Bionanotechnology. *Chem. Soc. Rev.* **2010**, *39*, 3499−3509.
(18) Hartgerink, J. D.; Beniash, E.; Stupp, S. I. Self-Assembly and Mineralization of Peptide−Amphiphile Nanofibers. *Science* **2001**, *294*, 1684−1688.
(19) Ghadiri, M. R.; Granja, J. R.; Milligan, R. A.; McRee, D. E.; Khazanovich, N. Self-Assembling Organic Nanotubes Based on a Cyclic Peptide Architecture. *Nature* **1993**, *366*, 324−327.
(20) Hardy, J.; Selkoe, D. J. The Amyloid Hypothesis of Alzheimer's Disease: Progress and Problems on the Road to Therapeutics. *Science* **2002**, *297*, 353−356.
(21) Luo, Z.; Zhang, S. Designer Nanomaterials Using Chiral Self-Assembling Peptide Systems and Their Emerging Benefit for Society. *Chem. Soc. Rev.* **2012**, *41*, 4736−4754.
(22) Amdursky, N.; Molotskii, M.; Aronov, D.; Adler-Abramovich, L.; Gazit, E.; Rosenman, G. Blue Luminescence Based on Quantum Confinement at Peptide Nanotubes. *Nano Lett.* **2009**, *9*, 3111−3115.
(23) Shi, J.; Du, X.; Yuan, D.; Haburcak, R.; Wu, D.; Zhou, N.; Xu, B. Enzyme Transformation to Modulate the Ligand−Receptor Interactions between Small Molecules. *Chem. Commun.* **2015**, *51*, 4899−4901.
(24) Jayawarna, V.; Smith, A.; Gough, J. E.; Ulijn, R. V. Three-Dimensional Cell Culture of Chondrocytes on Modified di-Phenylalanine Scaffolds. *Biochem. Soc. Trans.* **2007**, *35*, 535−537.
(25) Mahler, A.; Reches, M.; Rechter, M.; Cohen, S.; Gazit, E. Rigid, Self-Assembled Hydrogel Composed of a Modified Aromatic Dipeptide. *Adv. Mater.* **2006**, *18*, 1365−1370.
(26) Yan, C.; Pochan, D. J. Rheological Properties of Peptide-Based Hydrogels for Biomedical and Other Applications. *Chem. Soc. Rev.* **2010**, *39*, 3528−3540.
(27) Buerkle, L. E.; Rowan, S. J. Supramolecular Gels Formed from Multi-Component Low Molecular Weight Species. *Chem. Soc. Rev.* **2012**, *41*, 6089−6102.
(28) Adhikari, B.; Nanda, J.; Banerjee, A. Short Peptide Based Hydrogels: Incorporation of Graphene into the Hydrogel. *Soft Matter* **2011**, *7*, 9259−9266.
(29) Nanda, J.; Adhikari, B.; Basak, S.; Banerjee, A. Formation of Hybrid Hydrogels Consisting of Tripeptide and Different Silver Nanoparticle-Capped Ligands: Modulation of the Mechanical Strength of Gel Phase Materials. *J. Phys. Chem. B* **2012**, *116*, 12235−12244.
(30) Locke, A. K.; Cummins, B. M.; Abraham, A. A.; Cote, G. L. PEGylation of Concanavalin A to Improve Its Stability for an In Vivo Glucose Sensing Assay. *Anal. Chem.* **2014**, *86*, 9091−9097.
(31) Zheng, J.; Callahan, L. A. S.; Hao, J.; Guo, K.; Wesdemiotis, C.; Weiss, R. A.; Becker, M. L. Strain-Promoted Cross-Linking of PEG-Based Hydrogels via Copper-Free Cycloaddition. *ACS Macro Lett.* **2012**, *1*, 1071−1073.
(32) Gao, J.; Wang, H.; Wang, L.; Wang, J.; Kong, D.; Yang, Z. Enzyme Promotes the Hydrogelation from a Hydrophobic Small Molecule. *J. Am. Chem. Soc.* **2009**, *131*, 11286−11287.
(33) Li, Y.; Ding, Y.; Qin, M.; Cao, Y.; Wang, W. An Enzyme-Assisted Nanoparticle Crosslinking Approach to Enhance the Mechanical Strength of Peptide-Based Supramolecular Hydrogels. *Chem. Commun.* **2013**, *49*, 8653−8655.
(34) Garmo, Ø. A.; Davison, W.; Zhang, H. Effects of Binding of Metals to the Hydrogel and Filter Membrane on the Accuracy of the Diffusive Gradients in Thin Films Technique. *Anal. Chem.* **2008**, *80*, 9220−9225.
(35) Mantion, A.; Massüger, L.; Rabu, P.; Palivan, C.; McCusker, L. B.; Taubert, A. Metal−Peptide Frameworks (MPFs): "Bioinspired" Metal Organic Frameworks. *J. Am. Chem. Soc.* **2008**, *130*, 2517−2526.
(36) Pan, Y.; Gao, Y.; Shi, J.; Wang, L.; Xu, B. A Versatile Supramolecular Hydrogel of Nitrilotriacetic Acid (NTA) for Binding Metal Ions and Magnetorheological Response. *J. Mater. Chem.* **2011**, *21*, 6804−6806.
(37) Bush, M. F.; Oomens, J.; Saykally, R. J.; Williams, E. R. Effects of Alkaline Earth Metal Ion Complexation on Amino Acid Zwitterion Stability: Results from Infrared Action Spectroscopy. *J. Am. Chem. Soc.* **2008**, *130*, 6463−6471.
(38) Volkringer, C.; Marrot, J.; Férey, G.; Loiseau, T. Hydrothermal Crystallization of Three Calcium-Based Hybrid Solids with 2,6-Naphthalene- or 4,4′-Biphenyl-Dicarboxylates. *Cryst. Growth Des.* **2008**, *8*, 685−689.
(39) Gaharwar, A. K.; Peppas, N. A.; Khademhosseini, A. Nanocomposite Hydrogels for Biomedical Applications. *Biotechnol. Bioeng.* **2014**, *111*, 441−453.
(40) Goenka, S.; Sant, V.; Sant, S. Graphene-Based Nanomaterials for Drug Delivery and Tissue Engineering. *J. Controlled Release* **2014**, *173*, 75−88.
(41) Zheng, X.; Wu, D.; Su, T.; Bao, S.; Liao, C.; Wang, Q. Magnetic Nanocomposite Hydrogel Prepared by ZnO-initiated Photopolymerization for La (III) Adsorption. *ACS Appl. Mater. Interfaces* **2014**, *6*, 19840−19849.
(42) Zhang, S. M.; Greenfield, M. A.; Mata, A.; Palmer, L. C.; Bitton, R.; Mantei, J. R.; Aparicio, C.; de la Cruz, M. O.; Stupp, S. I. A Self-Assembly Pathway to Aligned Monodomain Gels. *Nat. Mater.* **2010**, *9*, 594−601.
(43) Ma, M.; Kuang, Y.; Gao, Y.; Zhang, Y.; Gao, P.; Xu, B. Aromatic−Aromatic Interactions Induce the Self-Assembly of Pentapeptidic Derivatives in Water To Form Nanofibers and Supramolecular Hydrogels. *J. Am. Chem. Soc.* **2010**, *132*, 2719−2728.
(44) Ding, Y.; Li, Y.; Qin, M.; Cao, Y.; Wang, W. Photo-Cross-Linking Approach to Engineering Small Tyrosine-Containing Peptide Hydrogels with Enhanced Mechanical Stability. *Langmuir* **2013**, *29*, 13299−13306.
(45) Turkevich, J.; Stevenson, P. C.; Hillier, J. A Study of the Nucleation and Growth Processes in the Synthesis of Colloidal Gold. *Discuss. Faraday Soc.* **1951**, *11*, 55−80.
(46) Frens, G. Controlled Nucleation for the Regulation of the Particle Size in Monodisperse Gold Suspensions. *Nature, Phys. Sci.* **1973**, *241*, 20−22.
(47) Yang, Z.; Liang, G.; Ma, M.; Gao, Y.; Xu, B. Conjugates of Naphthalene and Dipeptides Produce Molecular Hydrogelators with High Efficiency of Hydrogelation and Superhelical Nanofibers. *J. Mater. Chem.* **2007**, *17*, 850−854.
(48) Estroff, L. A.; Hamilton, A. D. Water Gelation by Small Organic Molecules. *Chem. Rev.* **2004**, *104*, 1201−1218.
(49) Wade, L. G., Jr. *Organic Chemistry*, 6th ed.; Pearson Prentice Hall: Upper Saddle River, NJ, 2006.
(50) Mantion, A.; Taubert, A. TiO_2 Sphere-Tube-Fiber Transition Induced by Oligovaline Concentration Variation. *Macromol. Biosci.* **2011**, *7*, 208−217.

DOI: 10.1021/acsami.5b05360
ACS Appl. Mater. Interfaces 2015, 7, 19306−19315